

Low Power and High Speed ALU using FinFET Technology

Shweta nagpal^[1], Amit sharma^[2],

Abstract: FinFET is a new device structure of vertical double gate and become the alternative device for the nanoscale design. In this paper, A One-Bit ALU is designed and simulated in 32nm technology using FinFET device technology. Simulation results indicate that the proposed technique provides improvement in Average Power Consumption and the use of FinFET device increases performance speed of the device logic.

Keywords: FinFET, ALU, MosFET, Adder

Introduction

As nanometer process technologies have advanced, chip density and operating frequency have increased, making power consumption in battery-operated portable devices a major concern. Even for no portable devices, power consumption is important because of the increased packaging and cooling costs as well as potential reliability problems. Thus, the main design goal for VLSI (very-large-scale integration) designers is to meet performance requirements within a power budget. [3] Therefore, power efficiency has assumed increased importance. This project explores how circuits based on FinFETs (fin-type field-effect transistors), an emerging transistor technology that is likely to supplement or supplant bulk CMOS) at 32-nm and beyond, offer interesting delay–power tradeoffs [7].

The desire to optimize the design metrics of performance, power, area, cost, and time to market (opportunity cost) has not changed since the inception of the IC industry. In fact, Moore's Law is all about optimizing those parameters. However, as scaling of manufacturing nodes progressed towards 20-nm, some of the device parameters could not be scaled any further, especially the power supply voltage, the dominant factor in determining dynamic power. [8] And optimizing for one variable such as performance automatically translated into big compromises in other areas, like power. Another limitation as processes approached 20-nm was the fact that lithography was stuck at ArF illumination source with a wavelength of 193nm while the process-critical feature was pushing sub-20nm. Optical innovations such as immersion lithography and double-attenuating made that possible, but at the cost of increased variability. [9] There were also other innovations along the way such as High-K metal gate that alleviated – to a limited extent – gate leakage problems. But the fact remained that the design window for optimizing among the aforementioned design variables was shrinking [1]. Designing in FinFET broadens the design window once again. [4] Operating voltage continues to scale down, significantly saving on dynamic and static power. Short channel effects are reduced significantly, reducing the guard-banding needed to deal with variability. [10] And performance continues to improve compared too planar at an identical node. In fact, at very low power supply voltages, the performance advantage of the FinFET compared to its planar equivalent widens due to the superior gate control of the channel in the FinFET. [5] For memory designers, an added advantage of FinFETs is the significantly lower retention voltage requirements of FinFET-based SRAMs compared to planar FETs. Given the emerging metric of performance per unit power (Koomey's Law), one major design optimization benefit of FinFET compared too planar is much higher performance at the same power budget, or equal performance at a much lower power budget. This essentially gives designers the ability to extract the highest performance for the lowest power, a critical optimization for battery-powered devices. [3] One feature that makes the transition from designing with planar FETs to

designing with FinFETs a little less complex is the fact that the back-end of the process is essentially the same, and therefore the part of the design flow associated with the physical implementation remains intact.

Scaling down the dimensions of MOSFETs is a continuous trend. The difficulties with reducing the size of the MOSFET include the semiconductor device fabrication process, the need for very low voltages, and with poorer electrical performance the necessity of circuit redesign and innovation [2]. It has been stated that smaller transistors switch faster, which is the main motivation for scaling down the dimensions of semiconductor devices [2].

1. FinFET Technology

FinFET is classified as a type of magnitude metal oxide semiconductor field effect transistor/MOSFET. It was first developed at the university of Berkley California by Chenning Hu and his colleagues

In FinFET the NMOS in CMOS technology is replaced with N-FinFET and PMOS with P-FinFET, then, both gates of FinFET are tied together. [7] By using this approach, we can design a FinFET version of a CMOS logic circuit or a pass transistor logic circuit that retains the same functionalities as the MOSFET version. [6] In the meantime, FinFET provides better circuit performances and reduces leakage current through effective suppression of short-channel effect and near-ideal sub-threshold swing [9].

In the single-gate mode, the short channel effects (threshold voltage roll-off, sub threshold swing degradation and drain induced barrier lowering) are actually less severe than those of the device in the double-gate mode [2].

2. ALU

ALU is known as heart of any processor or controller and is a most vital part of the system. It generally performs basic arithmetic and logical operations. The efficiency, speed and power consumption of a processor largely depends on the ALU. The demand for a high speed processing has been increasing as a result of expanding computer calculations and signal processing applications. Higher throughput efficiency arithmetic operations are important to achieve the desired performance in many real-time signal analysis and image processing application.

3. Proposed ALU Design using FinFETs

The ALU which is to be implemented performs arithmetic operations such as addition and logical operations such as AND & OR. It is basically a three function ALU.

The ALU consists of NAND, NOR, Inverter, Full Adder and a 4:1 Mux. It performs three functions depending on the values of select lines, S0 and S1.

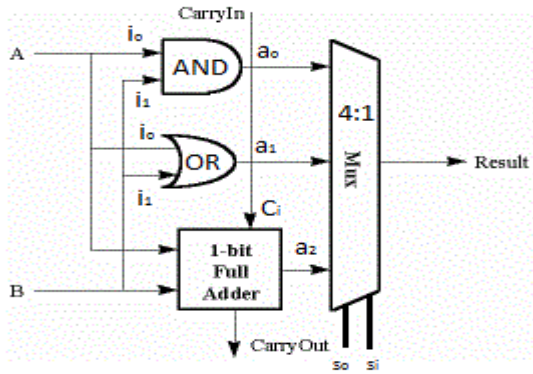


Figure 1: ALU Block Diagram

The logic circuits of AND, OR, Inverter, Full Adder and Multiplexer are made using CMOS logic, replacing the conventional MOSFETs with FinFETs.

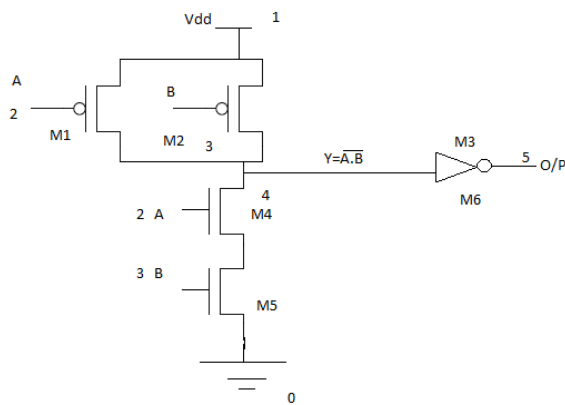


Figure 2: AND Gate

Figure 1 shows the block diagram of ALU, and the CMOS circuits with nodes naming of AND, OR and Full Adder are shown in Figure 2, 3 and 4 respectively.

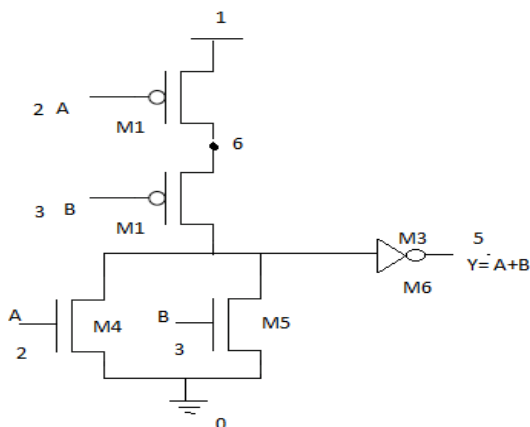
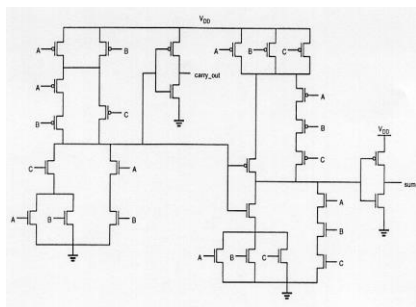


Figure 2: OR Gate

The transistor symbols used in the figure are of MosFET, FinFET symbols as studied in [3] is shown in figure 5. All the circuits are made in short gate configuration of FinFETs as shown in Figure 5.



| | OR MOSFET(nW) | OR FINFET(nW) |
|---------------|---------------|---------------|
| Average Power | 322 | 51.67 |

Figure 4: Full Adder

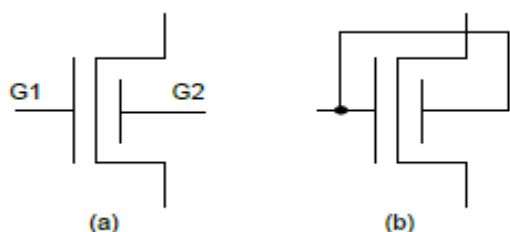


Figure 5: FinFET Configurations (a) Independent Gates (b) Shorted Gates [9]

The results are calculated on synopsis HSPICE by coding the nodes of the circuit diagram, the circuit diagram nodes are given different node name, for which the FINFET model from BSIMCMG is included and simulated. The 2-bit opcode selects the result of either logical or arithmetic block which will be the output of the ALU.

4. Simulation Results

The simulations performed in HSPICE are analyzed in this section. The table 1, 2 and 3 respectively show the Average power comparison in AND, OR and Full Adder respectively.

Table 1: Average Power AND Gate

| | AND MOSFET(nW) | AND FINFET(nW) |
|---------------|----------------|----------------|
| Average Power | 387 | 65.1 |

Table 2: Average Power OR Gate

| | Full Adder MOSFET(nW) | Full Adder FINFET(nW) |
|---------------|-----------------------|-----------------------|
| Average Power | 692 | 143 |

Table 3: Average Power Full Adder

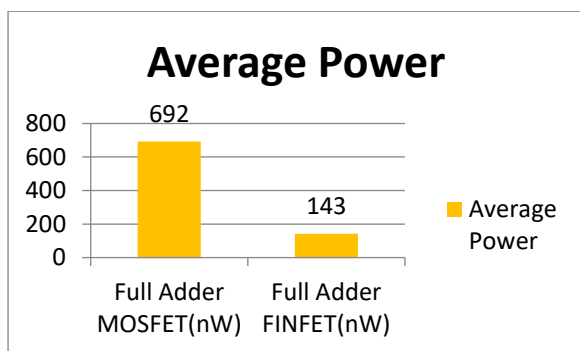


Figure 6: AND Gate Average Power

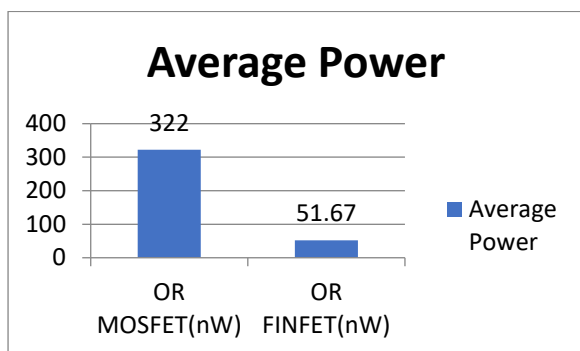


Figure 7: OR Gate Average Power

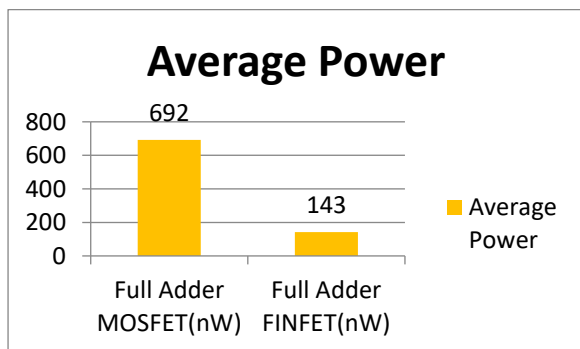
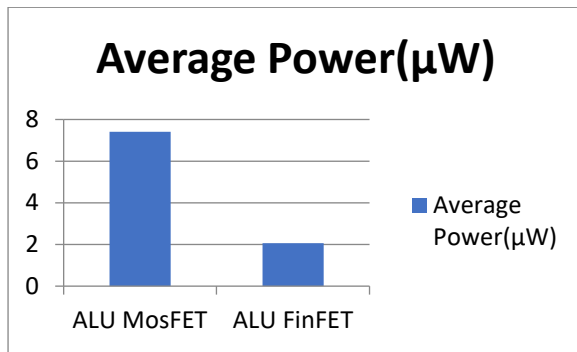


Figure 8: AND Gate Average Power

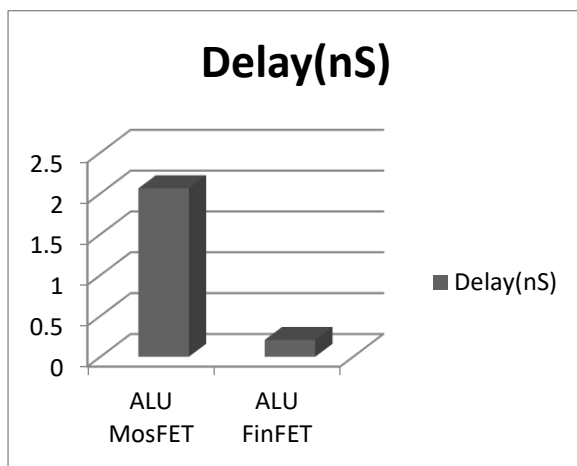
Figure 6, 7 and 8 are representing bar graphical representation of Average power consumption comparison in FinFET device circuit and MosFET device circuit. The results clearly prove that a lot of power saving and high efficiency can be achieved by the use of FinFET.

Figure 8: Average Power Consumption in ALU FinFET and ALU MosFET



The Figure 9 and 10 shows overall comparison of FinFET based ALU with MosFET based ALU. The model files of FinFET and MosFET are taken in 32nm technology from predictive technology models.

Figure 9: Delay in ALU FinFET and ALU MosFET



5. Conclusion

The use of FinFET over MOSFET in the proposed technique reduces average power consumption and delay in one bit ALU. The reduced short channel effects in FinFET and better control over the gate of the FinFET improves the average power delay in proposed technique. As already shown in simulation results, the Average Power Consumption and delay are greatly reduced in FinFET than MosFET. The MOSFET has been used widely in current technology. But below 32nm technology, controlling the channel of the MOSFET becomes difficult. So there is need to invent new technology which will allow us to design devices below 32nm technology.

6. References

- [1] Junki Kato, CES, 2014 “Circuit design of 2 i/p reconfigurable Dynamis Logic based on DG MOSFETs with whole set of 16 functions”
- [2] Zhichao Lu, IEEE, Vol 28, Feb- 2007, “Short Channel Effects in FinFet”
- [3] Ajay N. Bhoj and Niraj K. Jha, IEEE, 2013, “Design of Logic Gates and Flip-Flops in High-performance FinFet Technology”

[4] R.Rajprabu, IOSR-JVSP, Vol 2, Apr- 2013, "Performance analysis of CMOS and FinFet Logic"

[5] Sherif A.Tawfika, Elsevier, 2011, "FinFET domino logic with independent gate keepers "

[6] Mahender Veshala , IJEIT 2013, "Reduction of Short-Channel Effects in FinFET"

[7] V Narendar , IJCA, 2012 , "Design of High-performance Digital Logic Circuits based on FinFET Technology "

[8] PC Rajashree, ICIET-2014, "Deep Submicron 50nm CMOS Logic Design with FINFET"

[9] Tushar Surwadkar, IJETT-2014, "Upgrading the performance of VLSI Circuits using FinFETs"

[10] Sneha Arora, Umesh Dutta, Vipin Kumar Sharma, "A Noise Tolerant and Low Power Dynamic Logic Circuit Using FinFET Technology. 5 - Issue 12 (December - 2015), International Journal of Engineering Research and Applications (IJERA) , ISSN: 2248-9622 , www.ijera.com

Abstract: - In many areas of the globe, particularly in mild climates, the demand for air conditioning is quickly growing. The only equipment that consumes more electricity say 70 percent in household articles is air conditioners and refrigerators. Usually a conventional cooling technology is based on the electrically powered cooling scheme. These systems have several disadvantages: they involve elevated concentrations of primary energy consumption, and in many areas of the globe, particularly in mild climates, demand for air conditioning is quickly rising. In many areas of the globe, particularly in mild climates, the demand for air conditioning is quickly growing. The only equipment that consumes more electricity say 70 percent in household articles is air conditioners and refrigerators. The factors together with the adsorbent-adsorbate couple, the gadget design and the arrangement of the subsystems were chosen with great care for the effective operation of this gadget.

Keywords: - air conditioning, energy consumption, refrigerators, adsorbent-adsorbate, gadget, subsystems

Introduction: -

According to the International Refrigeration Institute, around 15 percent of the world's complete electricity generation is consumed for cooling and air conditioning purposes. Approximately 80% of the world's energy is produced through the use of fossil fuels that substantially increase CO₂ emissions, leading to an increase in worldwide warming [1]. The exploitation of current solar energy to run a refrigeration system is reasonable in order to decrease the consumption of fossil fuels and at the same moment encourage the use of sustainable energy. Using solar energy as the demand for cooling and the quantity of solar energy available are directly proportional to each other is quite viable [2]. Solar-driven vapor compression cooling has benefits in energy conservation and environmental protection, but standard solar-driven vapor compression cooling has many disadvantages, such as low effectiveness, intermittent operation, excessive unit size and excessive capital costs [3]. Most cooling systems work on the refrigeration cycle of vapor compression. This system generally consumes high-grade and dearer electrical power as well. Large-scale energy consumption from traditional resources such as fossil fuels also presents critical problems that need to be resolved with the utmost care and circumstances [5]. The on - the-spot mitigation

technique is to emphasize all electricity-invasive industries to make use of renewable energy resources that include sun energy, wind power, and so on as well as waste heat from business methods [6]. Different recognized commercial electricity assets, solar power is proven to be readily accessible for energy-hungry places in tropical areas (on our mother planet, the Earth). Although solar power is diluted and intermittent, its cooling urge is due to its abundant and non-polluting accessibility [7].

Proposed methodology:

On the premise of requirement and alertness of refrigeration, system components are designed thermally with the assist of heat switch evaluation alongside thermodynamic standards. the principle additives require right design of adsorption mattress, evaporator, capillary and condenser. the subsequent sections illustrate the numerous methodologies followed to estimate the required geometrical parameters of components of adsorption system working with selected working pairs.

Design of adsorption bed:

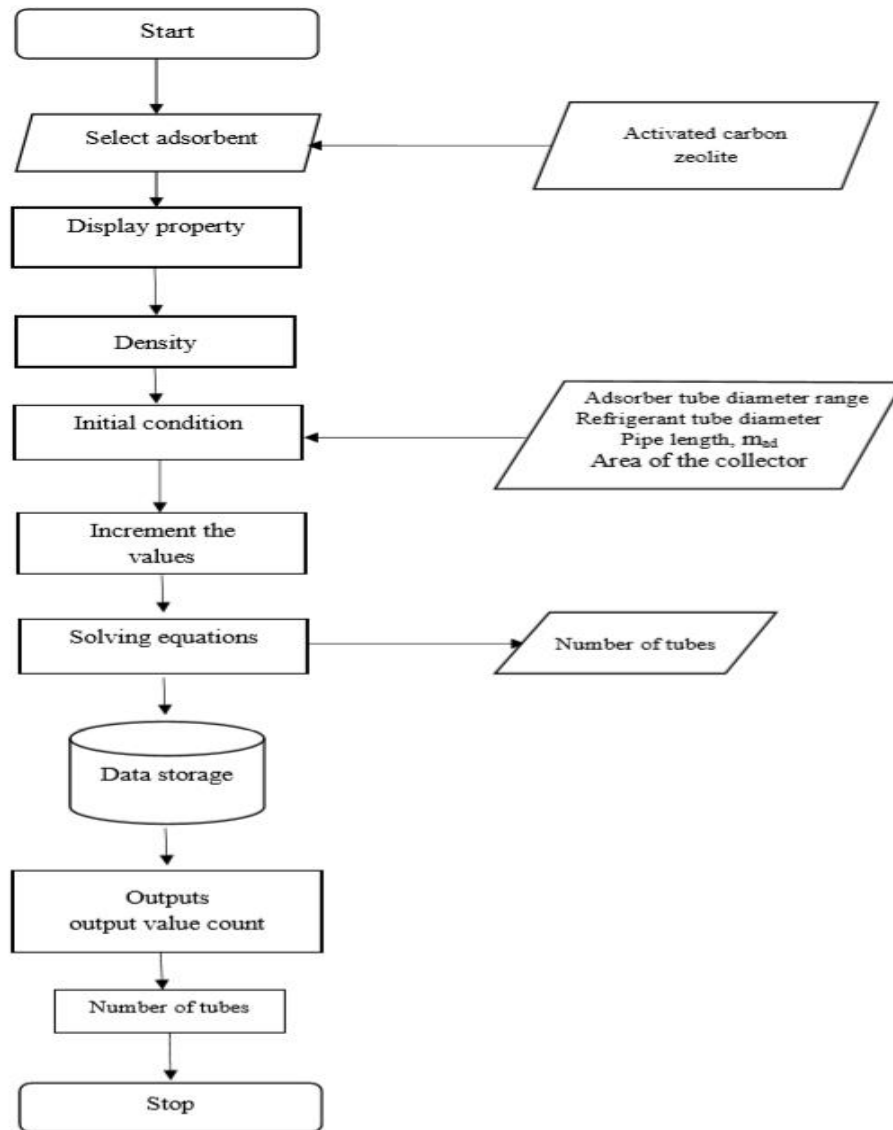


Figure 1: Algorithm of adsorption bed designer

The above figure 1 shows the Algorithm of adsorption bed designer.

Design of evaporator:

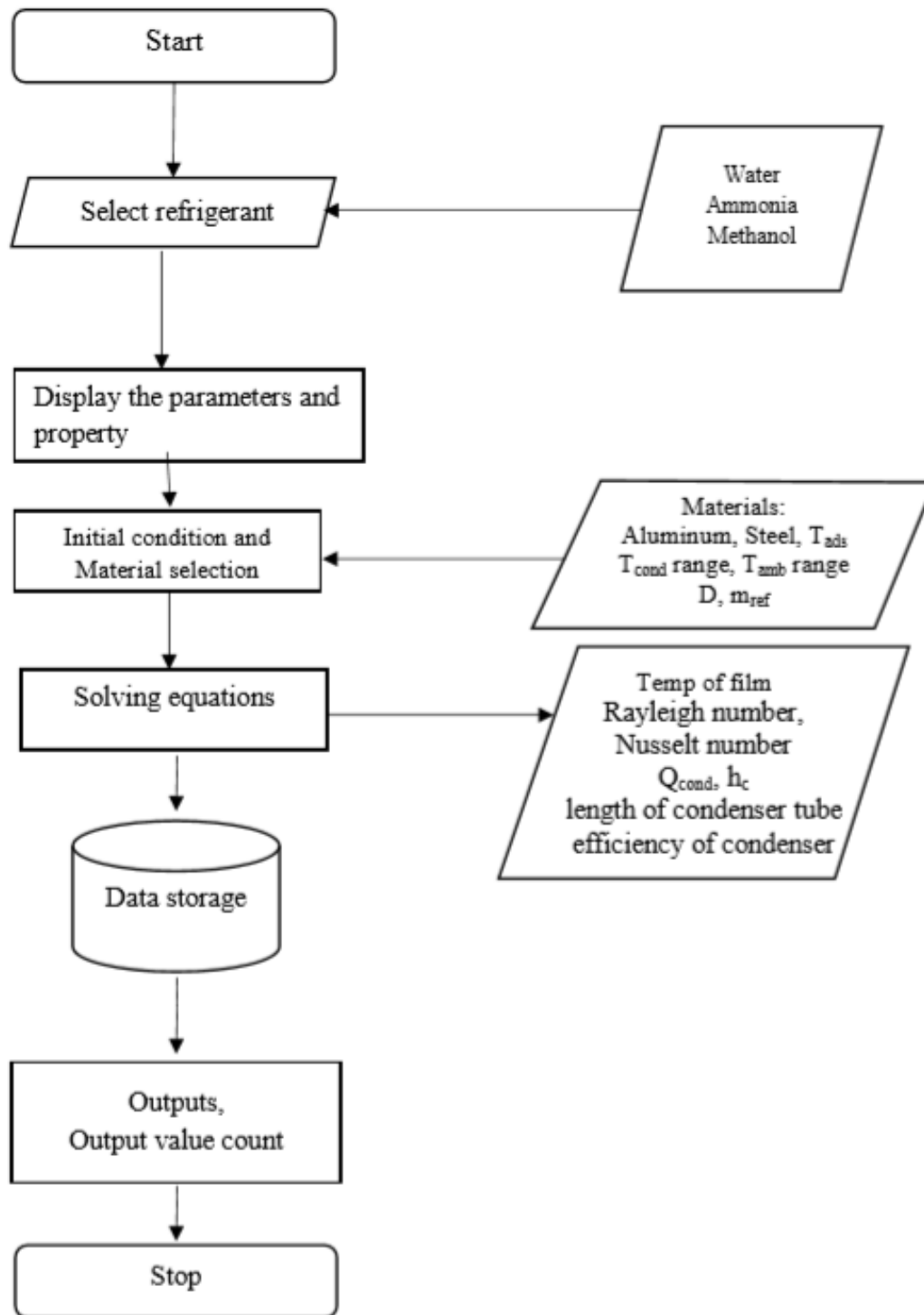


Figure 3: Algorithm of evaporator designer

The figure 3 shows the Algorithm of evaporator designer. The heat needs to be dissipated from the condenser should be accurately calculated to condense the refrigerant to the liquid within the prescribed period of time-shares optimiser condenser designer instrument is a helpful instrument for determining the length and diameter of the pipe needed for a particular implementation.

Result:

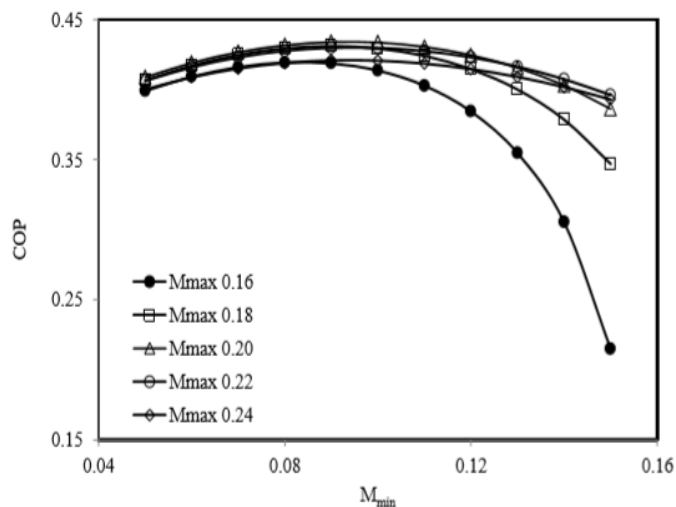


Figure 4: Influence of minimum mass concentration ratio on COP at $T_{evap}=274$ K, $T_{cond}=298$ K, $Q_{evap} =1000$ kJ/hr for zeolite-water

The above figure 4 shows the Influence of minimum mass concentration ratio on COP at $T_{evap}=274$ K, $T_{cond}=298$ K, $Q_{evap} =1000$ kJ/hr for zeolite-water

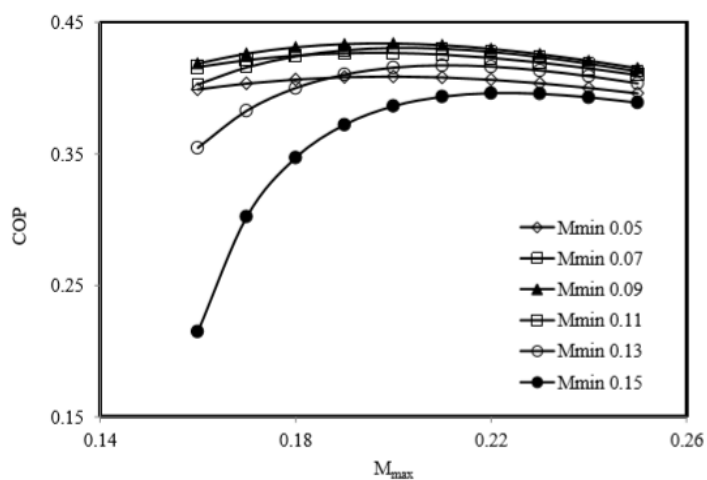


Figure 5: Influence of maximum mass concentration ratio on COP at $T_{evap}=274$ K, $T_{cond}=298$ K, $Q_{evap} =1000$ kJ/hr for zeolite-water

The above figure 5 shows the Influence of maximum mass concentration ratio on COP at $T_{evap}=274$ K, $T_{cond}=298$ K, $Q_{evap} =1000$ kJ/hr for zeolite-water.

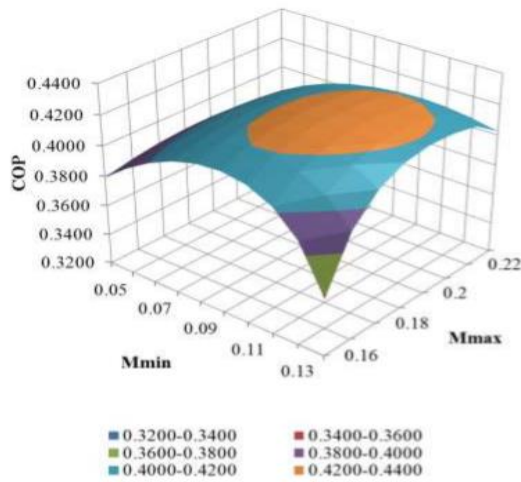


Figure 6: Effect of mass concentration ratios on COP for zeolite-water

The figure 6 shows the Effect of mass concentration ratios on COP for zeolite-water.

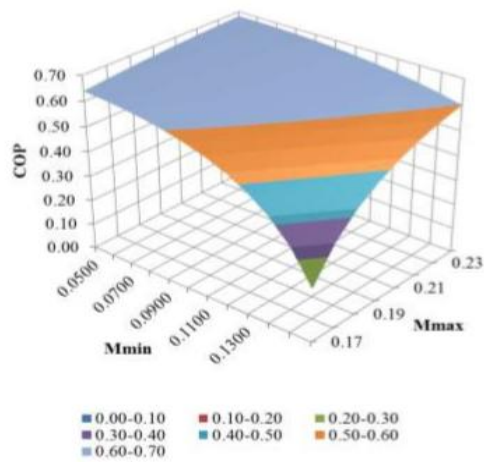


Figure 7: Effect of mass concentration ratios on COP for AC-methanol

The figure 7 shows the Effect of mass concentration ratios on COP for AC-methanol

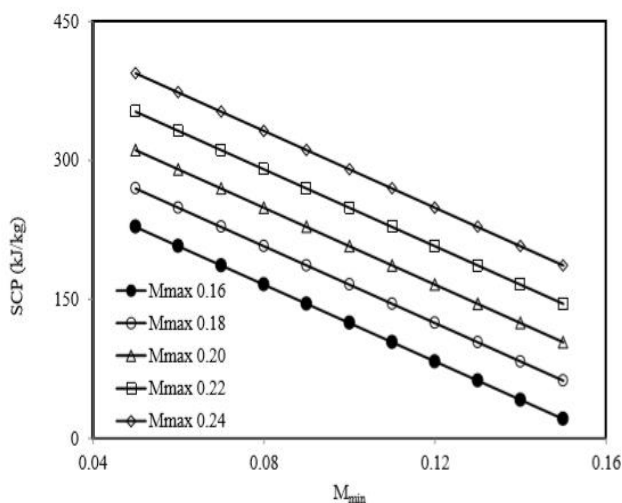


Figure 8: Influence of minimum mass concentration ratio on SCP at $T_{evap}=274$ K, $T_{cond}=298$ K, $Q_{evap} =1000$ kJ/hr -water

The figure 8 shows the Influence of minimum mass concentration ratio on SCP at $T_{evap}=274$ K, $T_{cond}=298$ K, $Q_{evap} = 1000$ kJ/hr for Zeolite-water

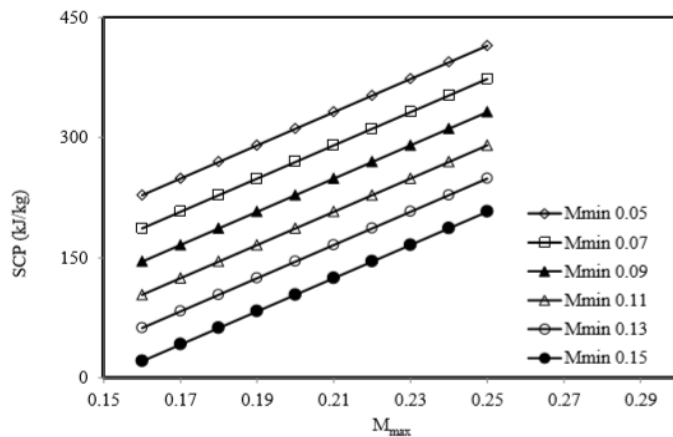


Figure 9: Influence of maximum mass concentration ratio on SCP at $T_{evap} = 274$ K $T_{cond} = 298$ K $Q_{evap} = 1000$ kJ/hr for Zeolite-water

The figure 9 shows the Influence of maximum mass concentration ratio on SCP at $T_{evap} = 274$ K $T_{cond} = 298$ K $Q_{evap} = 1000$ kJ/hr for Zeolite-water.

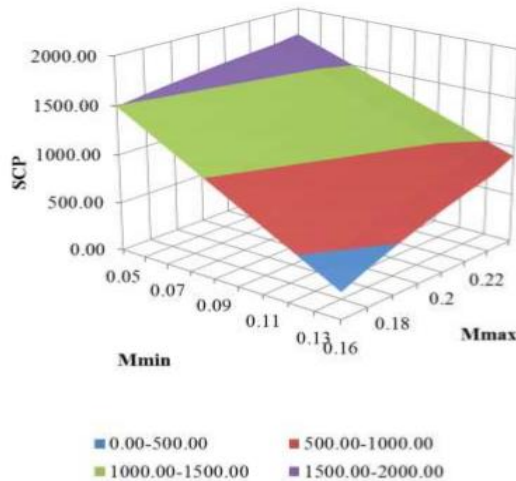


Figure 10: Influence of mass concentration ratios on SCP for Zeolite-water

The figure 10 shows the Influence of mass concentration ratios on SCP for Zeolite-water.

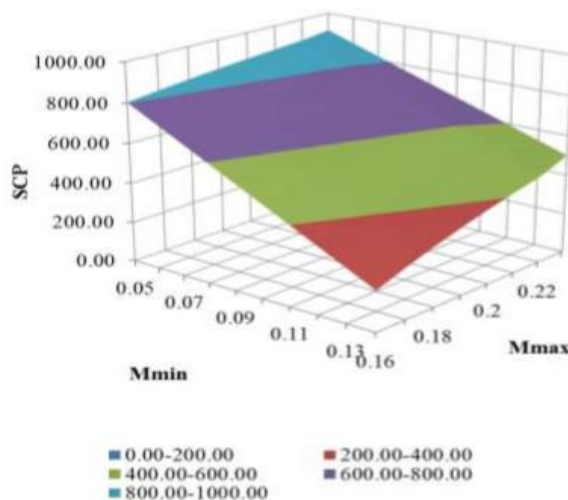


Figure 11: Influence of mass concentration ratios on SCP for AC-methanol

The figure 11 shows the Influence of mass concentration ratios on SCP for AC-methanol.

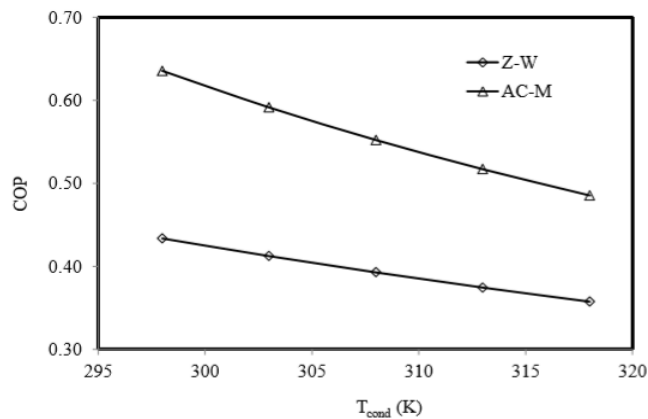


Figure 12: Influence of condenser temperature on COP for two different adsorption pairs for $T_{evap} = 274$ K, $M_{max} = 0.2$, $M_{min} = 0.1$, $Q_{evap} = 1000$ kJ/hr

The figure 12 shows the Influence of condenser temperature on COP for two different adsorption pairs for $T_{evap} = 274$ K, $M_{max} = 0.2$, $M_{min} = 0.1$, $Q_{evap} = 1000$ kJ/hr.

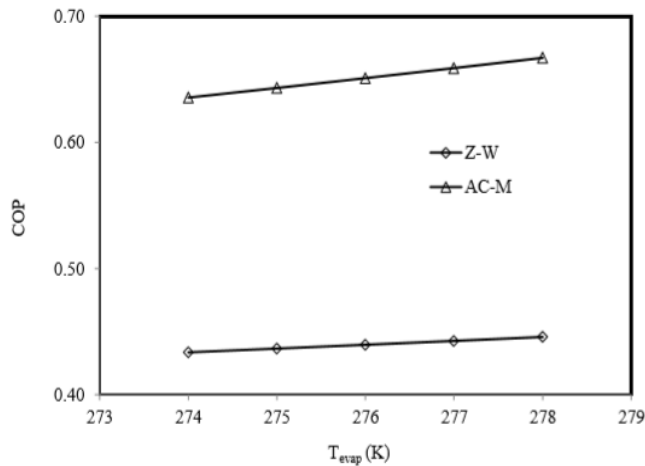


Figure 13: Influence of evaporator temperature on COP for different adsorption pairs. $T_{cond} = 298$ K, $M_{max} = 0.2$, $M_{min} = 0.1$, $Q_{evap} = 1000$ kJ/hr

The figure 13 shows the Influence of evaporator temperature on COP for different adsorption pairs. $T_{cond} = 298$ K, $M_{max} = 0.2$, $M_{min} = 0.1$, $Q_{evap} = 1000$ kJ/hr

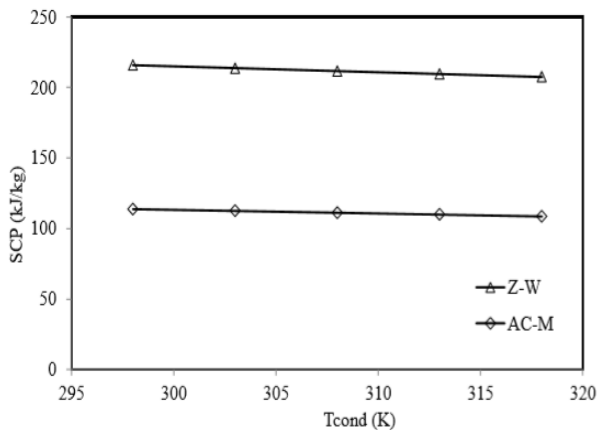


Figure 14: Outcome of condenser temperature on SCP of dissimilar adsorption pairs. $T_{evap} = 274$ K, $M_{max} = 0.2$, $M_{min} = 0.1$, $Q_{evap} = 1000$ kJ/hr

The figure 15 shows the Outcome of condenser temperature on SCP of different adsorption pairs. $T_{evap} = 274$ K, $M_{max} = 0.2$, $M_{min} = 0.1$, $Q_{evap} = 1000$ kJ/hr

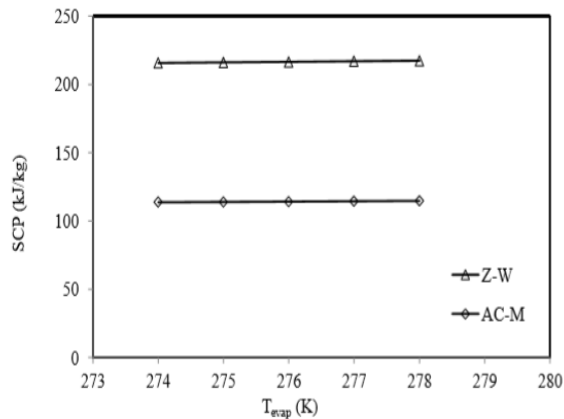


Figure 15: Outcome of evaporator temperature on SCP for dissimilar adsorption pairs. $T_{cond} = 298$ K, $M_{max} = 0.2$, $M_{min} = 0.1$, $Q_{evap} = 1000$ kJ/hr

The figure 15 shows the Effect of evaporator temperature on SCP for different adsorption pairs. $T_{cond} = 298$ K, $M_{max} = 0.2$, $M_{min} = 0.1$, $Q_{evap} = 1000$ kJ/hr

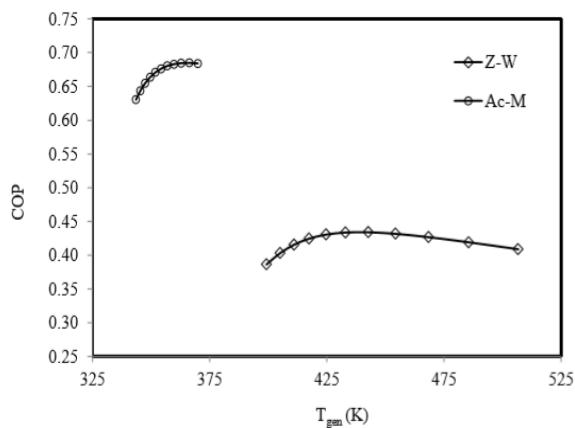


Figure 16: Consequence of generation temperature on COP for different adsorption pairs. $T_{evap} = 274$ K, $T_{cond} = 298$ K, $M_{max} = 0.2$, $Q_{evap} = 1000$ kJ/hr

The figure 16 shows the Consequence of generation temperature on COP for different adsorption pairs. $T_{evap} = 274$ K, $T_{cond} = 298$ K, $M_{max} = 0.2$, $Q_{evap} = 1000$ kJ/hr

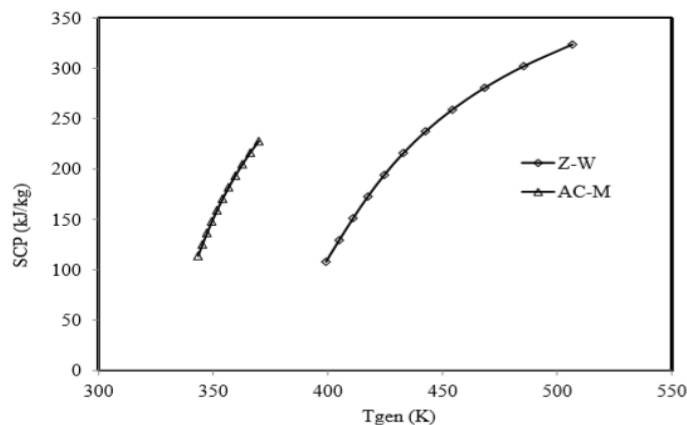


Figure 17: Consequence of generation temperature on SCP for different adsorption pairs.
 $T_{evap} = 274\text{ K}$, $T_{cond} = 298\text{ K}$, $M_{max} = 0.2$, $Q_{evap} = 1000\text{ kJ/hr}$

The figure 17 shows the Consequence of generation temperature on SCP for different adsorption pairs. $T_{evap} = 274\text{ K}$, $T_{cond} = 298\text{ K}$, $M_{max} = 0.2$, $Q_{evap} = 1000\text{ kJ/hr}$

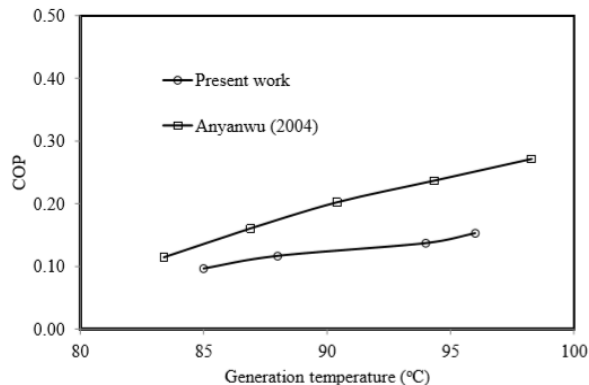


Figure 18: Validation of experimental results

The figure 18 shows the Validation of experimental results.

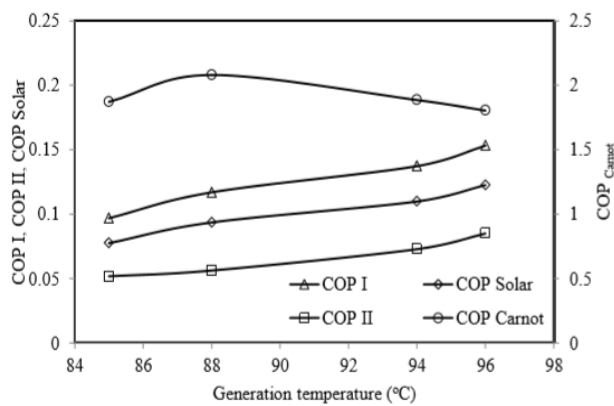


Figure 19: Plot of COP's vs generation temperature

The figure 4.23 shows Plot of COP's vs generation temperature

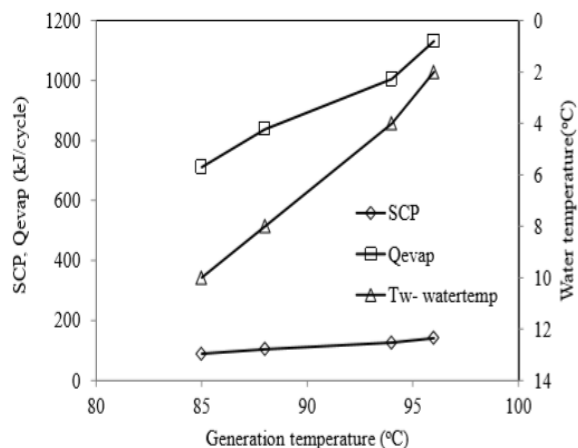


Figure 20: Variation of SCP, Qevap and Tw with generation temperature

The figure 20 shows Variation of SCP, Qevap and Tw with generation temperature

Conclusion: -

The design of the refrigeration adsorption gadget is promising. A general thermodynamic-based adsorption machine comparison indicates that the machine's efficiency depends on each of the pairs and procedures of adsorption. The generation continues to expand and the cost of sun adsorption refrigeration energy production is dropping. This article provides a typical evaluation of important knowledge of suitable housing of adsorbent pairs and methods engaged in the refrigeration cycle of adsorption. The proportion of temperatures, pressures and concentration was calculated at exclusive points. Furthermore, there were countless generation and absorber temperatures to determine the most effective temperatures.

References:

- [1] Ahmed M. Qenawy" Current Technologies and Future Perspectives in Solar Powered Adsorption Systems" Montreal, August 20-24, 2004
- [2] Kaushalendra Kumar Dubey "Thermodynamic (Energy-Exergy) Analysis of Combined Coal based Thermal Power Plant and Solar Integrated Double Bed Vapor Adsorption System for Heat Recovery and Space Cooling" Saudi J. Eng. Technol.; Vol-2, Iss-7(Jul, 2017):286-299.
- [3] Prof. B. A. Shah "Adsorption Refrigeration Technologies" AHMEDABAD – 382 481, 8-10 DECEMBER, 2011
- [4] V. Mittal" Performance evaluation of solar absorption cooling system" Received on July 29, 2005; Revised on September 12, 2005.
- [5] Rahul "Vapour Absorption Refrigeration System by using Solar Energy" Vol. 3, Issue 11, 2016 | ISSN (online): 2321-0613
- [6] Bipin Karki "Experimental and Life Cycle Analysis of a Solar Thermal Adsorption Refrigeration (Star) Using Ethanol - Activated Carbon" Dayton, Ohio May 2018
- [7] Sachin Kaushik "Thermodynamic Analysis of Vapor Absorption Refrigeration System and Calculation of COP" Vol. 2 Issue II, February 2014
- [8] Furio Caserta "Comparison between different solar cooling thermally driven system solutions for an office building in Mediterranean Area" Vol. 35, No. 1, March 2017, pp. 130-138
- [9] Amirhossein Sharafianardakani "Waste heat-driven adsorption cooling systems for vehicle air conditioning applications" 2015
- [10] Zi-Jie Chien "Experimental Investigation on an Adsorption Refrigerator Driven by Solar Cells" Received 23 November 2012; Accepted 7 January 2013